Membrane–Sugar Interactions Probed by Pulsed Electron Paramagnetic Resonance of Spin Labels

ARTICLE *in* THE JOURNAL OF PHYSICAL CHEMISTRY B · AUGUST 2015

Impact Factor: 3.3 · DOI: 10.1021/acs.jpcb.5b06864

THE JOURNAL OF PHYSICAL CHEMISTRY B

Article

pubs.acs.org/JPCB

Membrane–Sugar Interactions Probed by Pulsed Electron Paramagnetic Resonance of Spin Labels

Konstantin B. Konov,[†] Dmitry V. Leonov,[‡,§] Nikolay P. Isaev,[‡,§] Kirill Yu. Fedotov,[‡,§] Violeta K. Voronkova,[†] and Sergei A. Dzuba*[,‡,§]

[†]Zavoisky Physical-Technical Institute, Russian Academy of Sciences, Kazan 420029, Russia

[‡]Institute of Chemical Kinetics and Combustion, Russian Academy of Sciences, Novosibirsk 630090, Russia

[§]Novosibirsk State University, Novosibirsk, 630090, Russia

Supporting Information

ABSTRACT: Sugars can stabilize biological systems under extreme desiccation and freezing conditions. Hypothetical molecular mechanisms suggest that the stabilization effect may be determined either by specific interactions of sugars with biological molecules or by the influence of sugars on the solvating shell of the biomolecule. To explore membrane–sugar interactions, we applied electron spin echo envelope modulation (ESEEM) spectroscopy, a pulsed version of electron paramagnetic resonance (EPR), to phospholipid bilayers with spin-labeled lipids added and solvated by aqueous deuterated sucrose and trehalose solutions. The phospholipids were 1,2-dipalmitoyl-*sn*-glycero-3-phosphocholine (DPPC). The spin-labeled lipids were 1,2-dipalmitoyl-*sn*-glycero-3-phospho-(TEMPO)choline (T-PCSL), with spin-label TEMPO at the lipid polar headgroup. The deuterium ESEEM amplitude was calibrated using known concentrations of glassy deuterated sugar solvents. The data obtained indicated that the sugar concentration near the membrane surface obeyed a simple Langmuir model of monolayer adsorption, which assumes direct sugar-molecule bonding to the bilayer surface.

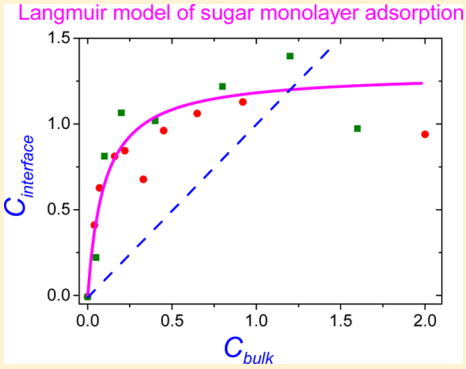

INTRODUCTION

Sugars are accumulated by many freezing-tolerant species.[1−3] The disaccharides sucrose and trehalose are known to stabilize cell membranes during freezing and dehydration.[4,5] However, the molecular mechanisms of this protective action are still a matter of debate. The existing literature models may be classified in several different ways;[6−20] however, all of them possess two distinctive features. One suggests that there are specific interactions between sugar molecules and the membrane surface that can stabilize the membrane structures, such as interlocking lipids headgroups.[6−12] The other assumes that sugars are not directly bonded to the membrane surface, and that their function is to stabilize the solvating shells upon freezing[13−17] by methods such as preventing ice formation in the intercellular liquid. The former may result in enhanced sugar concentration near the membrane surface (water replacement hypothesis), while the latter suggests that sugars are normally excluded from the bilayer surface (exclusion hypothesis). It has also been suggested that both models can be realized simultaneously: sugars may either be bound or expelled, depending on their concentration.[18−20] Note also that disaccharides are known to strongly influence protein dynamics in various biological processes (see refs 21 and 22).

To select between different mechanisms, experimental approaches allowing the direct detection of local sugar concentrations near the membrane surface are desirable. The spin-label electron paramagnetic resonance (EPR) technique can provide information at the molecular level on the structural and dynamical properties of biomolecules.[23−25] Electron spin echo envelope modulation (ESEEM)[26,27] spectroscopy, which is a pulsed version of EPR, allows the direct examination of the accessibilities of deuterium-substituted molecules to spin labels.[28−31]

The ESEEM phenomenon arises from the anisotropic hyperfine interactions between the unpaired electron of a spin label with nearby magnetic nuclei. The amplitude of the ESEEM depends on the distance to the nuclei and on the nuclei concentration. It decreases rapidly for distances greater than 0.5 nm,[32] which can be considered the spatial resolution of the method. The use of deuterium allows hydrogen atoms to be distinguished from the molecules under study and from the others in the surroundings.

In this work, we studied phospholipid bilayers prepared from 1,2-dipalmitoyl-*sn*-glycero-3-phosphocholine (DPPC). Bilayers were doped by 1,2-dipalmitoyl-*sn*-glycero-3-phospho-(TEMPO)choline (T-PCSL), in which spin-label TEMPO is attached to the lipid polar headgroup. In reference experiments, instead of T-PCSL, bilayers were doped by 1-palmitoyl-2-

Received: June 10, 2015
Revised: July 25, 2015

DOI: 10.1021/acs.jpcb.5b06864
J. Phys. Chem. B XXXX, XXX, XXX−XXX

stearoyl-(*n*-DOXYL)-*sn*-glycero-3-phosphocholine (*n*-PSPC, *n* optionally is 5 or 7), in which spin-label DOXYL is attached to the *n*th carbon atom of the acyl chain. Bilayers were prepared as multilamellar vesicles (MLV).

EXPERIMENTAL SECTION

Synthesis of Deuterated Sucrose and Trehalose. Deuterated sucrose and trehalose were prepared with a previously described method.[33] Briefly, 1 g of sugar (Sigma) was dissolved in 10 mL of D_2O, and then the solution was dried under evaporation. The residue was dissolved again in D_2O (20 mL), and 3 g of Raney nickel (SoyuzReakhim, Moscow) that had been stored previously for 24 h in 5 mL of D_2O was added. The mixture was heated under reflux for 10 h and then cooled. The Raney nickel was filtered off, and the filtrate was dried at 55 °C until the complete removal of the solvent was achieved. The resulting product was then mixed with an excess of normal water. The following evaporation of water resulted in the formation of the final product. NMR spectra were then recorded, which provided an average deuteration degree of 2.5 ± 0.5 and 6 ± 1 deuterium atoms per molecule for sucrose and trehalose, respectively. NMR data showed that the hydrogen in both sugars was replaced by deuterium in the positions where it is bonded to a carbon to which the hydroxyl group is also bonded.

Sample Preparation. DPPC and spin-labeled lipids T-PCSL, 5-PCSL, and 7-PCSL were obtained from Avanti Polar Lipids (Birmingham, AL). Their chemical structures are shown below:

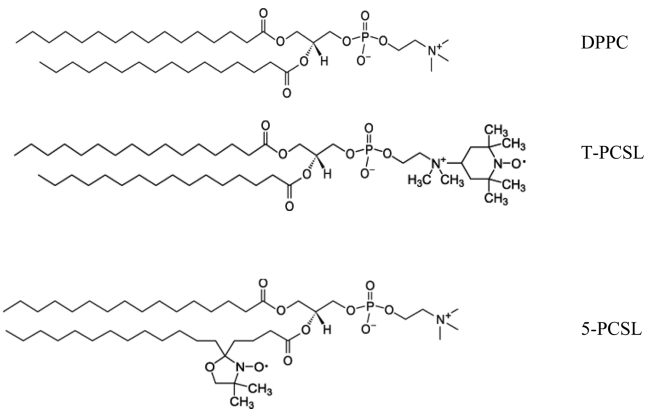

Note that 7-PCSL differs from 5-PCSL by label position.

Spin-labeled lipid (approximately of 0.5 mg) was dissolved in 2,2,2-trifluoroethanol (Sigma-Aldrich). DPPC was then added to this solution. After being mixed, the resulting solution was poured into 3 mm EPR tubes. The solvent was removed from the tubes by dry nitrogen gas flow and then stored under a 10^{-3} bar vacuum for 12 h. Aqueous solution of deuterated sugar was then added. The resulting samples contained 30 μg of spin-labeled lipid, 2.4 mg of DPPC (which makes an approximately 1/100 molar ratio of labeled and unlabeled lipids) and approximately 10 mg of sugar solution. The samples were stored at 60 °C for 3 h and then at 5 °C for 12 h. The samples were then placed into a refrigerator and stored at −20 °C.

For calibration purposes, solutions were also prepared in water or in a water−glycerol mixture (1:1 v/v) containing 1 mM nitroxide spin probe TEMPOL (a gift from Prof. I. A. Grigoriev; chemical structure is given below) and deuterated sugars of different concentrations.

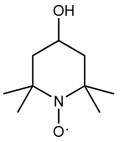

TEMPOL

CW EPR and ESEEM Measurements. All measurements were performed on an ELEXSYS E580 X-band EPR spectrometer (Bruker) using a dielectric resonator Bruker ER 4118 X-MD5 and a CF935 cryostat (Oxford Instruments). In continuous wave (CW) EPR experiments, the incident microwave power was controlled to prevent saturation of the EPR spectra. In pulse experiments, the cavity was overcoupled to provide a short ring time (approximately 100 ns). A low temperature was obtained using liquid nitrogen flow and controlled by an ITC 503S temperature controller (Oxford Instruments). All measurements were done at a temperature of 80 K.

ESEEM was obtained in a three-pulse sequence: $\pi/2-\tau-\pi/2-T\pi/2-\tau-$echo. The $\pi/2$ pulse durations were 16 ns. The τ interval was set to 200 ns, which is optimal for maximizing the deuterium and reducing the hydrogen ESEEM amplitude. The spectrometer magnetic field was set to the maximum of the echo-detected EPR spectrum. The ESEEM time traces were obtained with a scanning time delay T with a 12 ns time step, from 248 ns to approximately 12 μs. Unwanted echoes at short delays were removed by a four-step phase cycling.

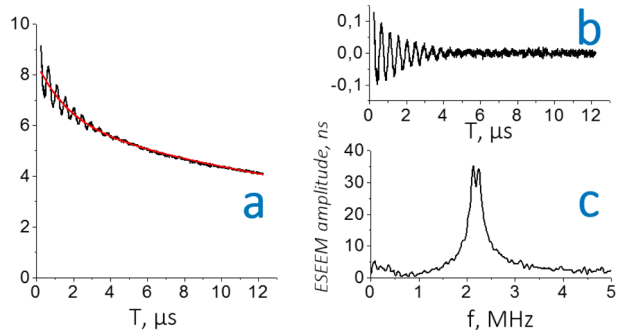

Figure 1. (a) Example of original ESEEM $V(T)$ time traces for a spin label in deuterated surroundings with the fitted smooth function $\langle V(T)\rangle$. (b) The $V_N(T)$ time-trace obtained using eq 1; (c) The result of the amplitude-value Fourier transformation eq 2. The sample is 1 mM TEMPOL dissolved in aqueous 1.6 M sucrose solution.

Data Treatment. The experimental time traces $V(T)$ were fitted by a smooth biexponential function (see Figure 1a) $\langle V(T)\rangle$ and then normalized as

$$V_N(T) = \frac{V(T)}{\langle V(T)\rangle} - 1 \quad (1)$$

The numerical amplitude-value Fourier spectra of $V_N(T)$ were then obtained:

$$F(f) = \left| \int_{t_1}^{t_2} V_N(t) \exp(-2\pi i f t) dt \right| \quad (2)$$

where $t = \tau + T$, τ = 200 ns, t_1 = 448 ns, t_2 = 12 μs, and f is the frequency in MHz. A custom computer program for Fourier transformations was used. Note that the spectral density $F(f)$

DOI: 10.1021/acs.jpcb.5b06864
J. Phys. Chem. B XXXX, XXX, XXX−XXX

has dimensions of time and does not depend on the incoming $V(T)$ signal intensity.

The resulting $F(f)$ shows an intensive peak at 2.2 MHz (see Figure 1c), which is the deuterium Larmor frequency in the spectrometer magnetic field used (340 mT). The peak is split into a doublet because of hyperfine and quadrupole interactions.[28,32] Below, the amplitude of this peak is referred to as the ESEEM amplitude.

RESULTS

Spin-Probe TEMPOL in Water and Water–Glycerol Solutions of Deuterated Sugars. Figure 2 presents the CW EPR spectra of spin-probe TEMPOL in aqueous deuterated sucrose solutions of different concentrations. Similar EPR spectra were obtained also for an aqueous trehalose solution and for a solution in a water–glycerol mixture (data not given). One can see that the EPR spectra in Figure 2 are practically

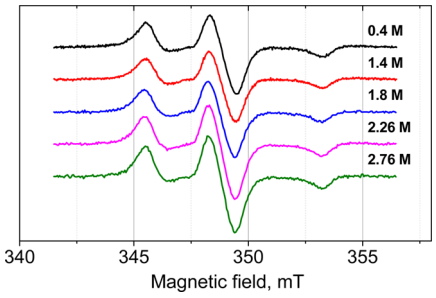

Figure 2. CW EPR spectra of 1 mM TEMPOL dissolved in aqueous sucrose solution of different molar concentrations. Spectra are vertically shifted for convenience.

independent of the sugar concentration. For aqueous sugar solutions, this result is important, considering that the samples appear to belong to different phase states: below 2.0 M, the samples were frozen as an opaque white powder, while near and above 2.0 M, the samples were transparent glasses. If guest TEMPOL molecules form a separate phase upon crystallization, severe distortion of the EPR line is expected because of aggregation. However, the data in Figure 2 show that this is not the case in the full concentration range studied. Therefore, one may conclude that even in the macroscopically crystalline phase of the aqueous sugar solution, the guest TEMPOL molecules are entrapped in a glassy molecular shell;[34] the apparent crystalline state of the sample may appear because of the formation of ice crystals in the amorphous surroundings.

Figure 3 shows the ESEEM amplitude for the TEMPOL spin probe dissolved in solutions of deuterated sugar in water and water-glycerol mixtures as a function of sugar concentration. For solutions in a water-glycerol mixture, the concentration dependencies are linear for both sugars. For aqueous sugar solutions, the whole range of concentrations can be divided into three regions: (i) below 1.4 M of sucrose and below 1.1 M of trehalose concentration, the ESEEM amplitude does not depend on concentration, (ii) between these values and 2 M for both sugar concentrations, the ESEEM amplitude decreases with concentration, and (iii) above 2 M for sucrose, the amplitude increases linearly with concentration (trehalose is insoluble above 2 M). As mentioned, the samples were transparent glasses at sugar concentrations near and above 2 M. So, the linear dependence above 2 M (for sucrose) may be related to the glassy state of the sample. The straight dashed

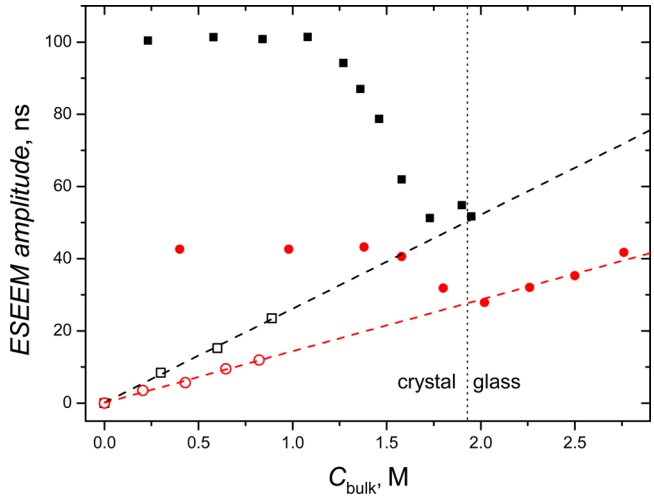

Figure 3. ESEEM amplitude for spin-probe TEMPOL taken as a function of the concentration of deuterated sugars in a water–glycerol mixture (empty symbols) and in water (filled symbols). Circles: samples with sucrose; squares: samples with trehalose. For water–glycerol solutions, the samples were transparent glasses; the dotted line indicates (for aqueous sugar solutions) the boundary for the formation of transparent glass. The dashed lines are linear extrapolations of data for the water–glycerol mixture.

lines in Figure 3 show that data for glassy aqueous sugar solutions coincide with linear extrapolation of data for glassy solutions in a water-glycerol mixture. This coincidence could imply that for both types of glass, the sugar molecules are similarly distributed around the spin-probe TEMPOL.

The tangent of the angle between these lines and the vertical axis is equal to 0.070 M/ns in the case of sucrose and 0.038 M/ns in the case of trehalose. Note that the proportion of these two values approximately corresponds to the NMR data obtained on the degree of deuteration (see the Experimental section). We used the obtained linear dependencies to calibrate the transformation of the measured deuterium ESEEM amplitude into local sugar concentration (that is, the sugar concentration in the area approximately 0.5 nm surrounding of the spin label[32]).

Spin-Labeled DPPC Bilayers in Aqueous Solutions of Deuterated Sugars. CW EPR spectra of spin-labeled lipids in DPPC bilayers hydrated in aqueous solutions of deuterated sucrose and trehalose were similar to those presented in Figure 2, and they also did not change with changing sugar concentration. The original ESEEM data are given in the Supporting Information. Note that amplitude-value Fourier transformation spectra, in addition to the deuterium-induced peaks at 2.2 MHz, also contain peaks at 1.0 MHz, with the amplitude independent of the sugar content (see spectra in the Supporting Information). Because 1.0 MHz exactly corresponds to the ^{14}N Larmor frequency in the magnetic field used (340 mT), these peaks may be unambiguously ascribed to interactions with the nitrogen of the choline group in the T-PCSL structure.

Figure 4 shows the ESEEM amplitude for T-PCSL (filled symbols) as a function of the bulk sugar concentration in solution, C_{bulk}. The original ESEEM amplitudes were recalculated using the empirical linear relations between sugar concentrations and the ESEEM amplitudes (i.e., multiplied by a factor of 0.070 M/ns in the case of sucrose and by a factor of 0.038 M/ns in the case of trehalose; see above) and then

DOI: 10.1021/acs.jpcb.5b06864
J. Phys. Chem. B XXXX, XXX, XXX–XXX

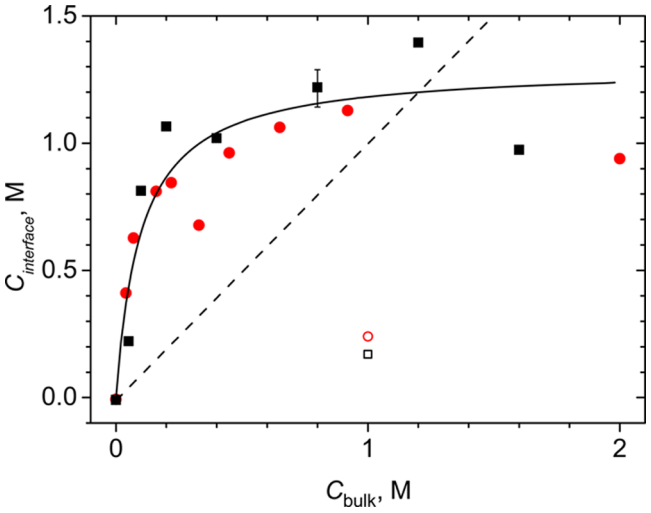

Figure 4. Sugar concentration in the solvation shell of the bilayer, $C_{inteface}$ (filled symbols), recalculated from the ESEEM amplitude for T-PCSL (see text for details), as a function of the bulk sugar concentration. Circles: samples with sucrose; squares: samples with trehalose. The typical experimental uncertainty is shown by bars. For comparison, the concentrations recalculated from the ESEEM data for 5-PCSL are also given as empty symbols (note that for 7-PCSL, the data are close). The solid line corresponds to the best-fit Langmuir isotherm (eq 3); the dashed line indicates the bisectrix of the right angle.

additionally multiplied by a factor of 2. The latter multiplication is done because the previous experiments for T-PCSL in a DPPC bilayer solvated by a glassy water–glycerol-d_5 mixture[35] showed that the ESEEM amplitude becomes twice as low in comparison to that with the spin label in the bulk. This diminishing of the ESEEM amplitude has an obvious explanation: that the spin label located at the membrane surface experiences interaction only with the half-space of deuterated media. Indeed, the results of analogous measurements for the DPPC bilayers doped with *n*-PCSL (n = 5 or 7) instead of T-PCSL show that the ESEEM amplitudes for *n*-PCSL are remarkably smaller than those for T-PCSL (see Figure 4). As in 5-PCSL and 7-PCSL, spin labels are located in the bilayer interior, while in T-PCSL, the spin labels are on the membrane surface; this difference implies that sugars do not penetrate into the membrane interior.

The resulting concentration, $C_{interface}$, is believed to refer to the local concentration of sugar in the solvation shell of the bilayer. For both sugars, data in Figure 4 show a sharp increase at small concentrations followed by a weaker dependence at larger concentrations. The weaker dependence indicates saturation behavior. For both sugars, ESEEM amplitudes are in quantitative mutual agreement. The dashed line in Figure 4 shows a putative situation when concentrations in the solvation shell and the bulk coincide.

The solid curve in Figure 4 corresponds to a theoretical expression for the Langmuir model of monolayer adsorption on the surface (Langmuir isotherm):

$$C_{interface} = C^{max}_{interface}\frac{KC_{bulk}}{1 + KC_{bulk}} \quad (3)$$

where $C^{max}_{interface}$ is maximal value for $C_{interface}$, and K is the ratio of adsorption and desorption rates. As the experimental data for both sugars in Figure 4 coincide within the experimental uncertainty, both data sets were fitted simultaneously. The best-fitted parameters were found to be $C^{max}_{interface}$ = 1.3 M and K = 10.0 M^{-1}.

DISCUSSION

The sharp initial increase in sugar concentration in the solvation shell of the bilayer, $C_{interface}$, compared with that in the bulk solution, C_{bulk}, is evidence that sucrose and trehalose accumulate near the surface (see Figure 4). It is interesting that this behavior obeys the simple theoretical Langmuir model of the monolayer adsorption on the surface. The important consequence of this fact is that adsorption implies direct interaction with the surface. The saturation behavior seen in Figure 4 at large bulk sugar concentrations (that can be assigned to sugar exclusion) is merely a consequence of the occupation of a monolayer at the membrane surface.

Note also a decrease of $C_{interface}$ at large bulk concentrations, seen in Figure 4. The reason for this decrease is unclear. More complicated models of molecular adsorption, such as the Langmuir–Freundlich model, also can fit the experimental results in Figure 4 but cannot explain this decrease.

The maximal sugar/lipid ratio in the solvation shell of the bilayer could be easily evaluated from the assessment of $C_{interface}$ = 1.3 M. Given that the lipid density in the bilayer is nearly of the same value, one sugar molecule near the membrane surface then corresponds to one lipid in the bilayer. Note that molecular dynamics (MD) simulations of membrane–trehalose interactions[20] for the 1,2-dimyristoyl-*sn*-glycero-3-phosphocholine (DMPC) bilayer led to the same conclusion that one trehalose molecule at the bilayer surface is bound to one lipid polar head.

Data on the concentration dependence given in Figure 4 are in general agreement with the results obtained for the net affinity of sugars for unilamellar DMPC bilayers,[19] which show that the effect reaches a maximum at a sugar concentration of 0.2 M. At concentrations larger than 0.2 M, the sugars were found to be gradually expelled from the membrane surface.[19] This is again in agreement with the data in Figure 4, which show that the saturation is attained just at the 0.2 M sugar concentration.

The location of sugars within a bilayer membrane was studied by small-angle neutron scattering, small-angle X-ray scattering,[13−15] and neutron diffraction.[17] It was shown that trehalose distribution follows a Gaussian profile centered in the water layer between bilayers.[17] It was concluded that trehalose is excluded from the membrane, and that its protective effects are determined largely by their nonspecific osmotic and volumetric effects.[17] In our opinion, the results of the present work do not contradict these data. Indeed, the 0.5 nm resolution of the ESEEM technique implies that data in Figure 4 refers to a thin monolayer near the membrane surface only, which could be beyond the spatial resolution of the neutron diffraction method. Additionally, sugars might be expelled from the membrane surface, as was observed in neutron diffraction,[17] with the exception of the first solvation layer.

Molecular motion for nearly the same system was studied by ESE (using spin-labeled stearic acids).[36] At low temperatures, stochastic orientational vibrations of the spin-labeled molecule as a whole (stochastic molecular librations or diffusive molecular wobbling) were found above 170–200 K in the case of solvation by pure water. This onset of motions at these temperatures is ascribed to the dynamical transition known for molecular glasses and the biological systems from neutron-

DOI: 10.1021/acs.jpcb.5b06864
J. Phys. Chem. B XXXX, XXX, XXX−XXX

scattering studies.[37] However, for the solvation by aqueous solutions of sucrose and trehalose, the onset of stochastic molecular librations was also found at lower temperatures near 120 K, which was explained by the bilayer expanding due to the direct bonding of sugar molecules to the bilayer surface. This result is in full agreement with the present conclusions made from ESEEM data.

The Langmuir adsorption model assumes that sugars are directly bonded to the bilayer surface, which is in favor of the water replacement hypothesis. However, if sugars near the membrane are present only in a thin monolayer, their possible stabilizing effect may not be enough to prevent damage to membranes upon freezing. Another important mechanism of the cryoprotective action of sugars could be the vitrification of the solvating shell of the membrane, which was proposed in number of works.[1−5,12−20] Spin-label EPR data are in agreement with this suggestion. Indeed, the vitrification of the solvation shell follows from the CW EPR spectra, which are typical for the glassy state (see above). Also, the temperature dependence of molecular motions of spin labels found previously in the bilayers[36] exhibits a dynamical transition typical for glassy state.

Note that the Langmuir adsorption model, along with the proposed glassy state of the membrane solvation shell, assumes phase separation leading to a membrane/sugar/water phase in equilibrium with a sugar/water phase at a different concentration that was previously proposed.[13−15,17]

CONCLUSIONS

We probed the interactions between the disaccharides sucrose and trehalose and a phospholipid DPPC bilayer surface. The spin-labeled pulsed EPR experimental approach allowed for the direct determination of the concentration of deuterated sugars in the immediate surroundings of spin labels in the bilayer, with a space resolution of approximately 0.5 nm. The amplitude of the ESEEM signal for the spin label at the surface as a function of sugar concentration was found to increase sharply at concentrations up to 0.2 M, with subsequent saturation behavior. The experimental dependence can be satisfactorily described by a Langmuir model of the monolayer adsorption. For this model, the maximal concentration near the surface and the ratio of rates for adsorption and desorption were found to be 1.3 and 10 M^{-1}, respectively. These results indicate that sugars are directly bonded to the bilayer surface (one sugar molecule per lipid), which is in favor of the water replacement hypothesis. Meanwhile, the glassylike behavior observed in this work and previous spin-label EPR results[36] are in agreement with the hypotheses, acknowledging the importance of vitrification of the solvation shell of the membrane.

The approach developed here could be used also to study membrane−peptide interactions, which is important for the elucidation of the molecular mechanisms of action of pore-forming peptide antibiotics.[30,31,38]

ASSOCIATED CONTENT

Supporting Information

The Supporting Information is available free of charge on the ACS Publications website at DOI: 10.1021/acs.jpcb.5b06864.

Original ESEEM $V_N(T)$ time traces along with the results of amplitude Fourier transformation for T-PCSL spin-labeled lipids in DPPC bilayers hydrated in aqueous solutions of deuterated sucrose and trehalose. (PDF)

AUTHOR INFORMATION

Corresponding Author

*E-mail: dzuba@kinetics.nsc.ru.

Notes

The authors declare no competing financial interest.

ACKNOWLEDGMENTS

The authors are thankful to N. E. Polyakov and M. Y. Volkov for NMR measurements. This work was supported by the Russian Science Foundation project no. 15-15-00021. Authors K.B.K. and D.V.L. contributed equally to this work.

REFERENCES

(1) Crowe, L. M. Lessons from Nature: The Role of Sugars in Anhydrobiosis. *Comp. Biochem. Physiol., Part A: Mol. Integr. Physiol.* **2002**, *131*, 505−513.
(2) Somero, G. N. Adapting to Water Stress: Convergence on Common Solutions. In *Water and Life*; Somero, G. N.; Osmond, C. B. and Bolis, C. L., Eds.' Springer: Berlin, 1992.
(3) Gilles, R. Compensatory"Organic Osmolytes in High Osmolarity and Dehydration Stresses: History and Perspectives. *Comp. Biochem. Phys. A* **1997**, *117*, 279−290.
(4) Crowe, J. H.; Carpenter, J. F.; Crowe, L. M. The Role of Vitrification in Anhydrobiosis. *Annu. Rev. Physiol.* **1998**, *60*, 73−103.
(5) He, X. M.; Fowler, A.; Toner, M. Water Activity and Mobility in Solutions of Glycerol and Small Molecular Weight Sugars: Implication for Cryo- and Lyopreservation. *J. Appl. Phys.* **2006**, *100*, 074702.
(6) Leekumjorn, S.; Sum, A. K. Molecular Investigation of the Interactions of Trehalose With Lipid Bilayers of DPPC, DPPE and their Mixture. *Mol. Simul.* **2006**, *32*, 219−230.
(7) Luzardo, M. D.; Amalfa, F.; Nuñez, A. M.; Díaz, S.; Biondi De Lopez, A. C.; Disalvo, E. A. Effect of Trehalose and Sucrose on the Hydration and Dipole Potential of Lipid Bilayers. *Biophys. J.* **2000**, *78*, 2452−2458.
(8) Villarreal, M. A.; Diaz, S. B.; Disalvo, E. A.; Montich, G. G. Molecular Dynamics Simulation Study of the Interaction of Trehalose with Lipid Membranes. *Langmuir* **2004**, *20*, 7844−7851.
(9) Lambruschini, C.; Relini, A.; Ridi, A.; Cordone, L.; Gliozzi, A. Trehalose Interacts with Phospholipid Polar Heads in Langmuir Monolayers. *Langmuir* **2000**, *16*, 5467−5470.
(10) Skibinsky, A.; Venable, R. M.; Pastor, R. W. A Molecular Dynamics Study of The Response of Lipid Bilayers and Monolayers to Trehalose. *Biophys. J.* **2005**, *89*, 4111−4121.
(11) Lairion, F.; Disalvo, E. A. Effect of Trehalose on the Contributions to the Dipole Potential of Lipid Monolayers. *Chem. Phys. Lipids* **2007**, *150*, 117−124.
(12) Golovina, E. A.; Golovin, A.; Hoekstra, F. A.; Faller, R. Water Replacement Hypothesis in Atomic Details: Effect of Trehalose on the Structure of Single Dehydrated POPC Bilayers. *Langmuir* **2010**, *26*, 11118−11126.
(13) Lenné, T.; Bryant, G.; Garvey, C. J.; Keiderling, U.; Koster, K. L. Location of sugars in multilamellar membranes at low hydration. *Phys. B* **2006**, *385−386*, 862−864.
(14) Lenné, T.; Garvey, C. J.; Koster, K. L.; Bryant, G. Effects of Sugars on Lipid Bilayers During Dehydration − SAXS/WAXS Measurements and Quantitative Model. *J. Phys. Chem. B* **2009**, *113*, 2486−2491.
(15) Kent, B.; Garvey, C. J.; Lenné, T.; Porcar, L.; Garamus, V. M.; Bryant, G. Measurement of Glucose Exclusion from the Fully Hydrated DOPE Inverse Hexagonal Phase. *Soft Matter* **2010**, *6*, 1197−1202.
(16) Söderlund, T.; Alakoskela, J-M. I.; Pakkanen, A. L.; Kinnunen, P. K. J. Comparison of the Effects of Surface Tension and Osmotic Pressure on the Interfacial Hydration of a Fluid Phospholipid Bilayer. *Biophys. J.* **2003**, *85*, 2333−2341.
(17) Kent, B.; Hunt, T.; Darwish, T. A.; Hauß, T.; Garvey, C. J.; Bryant, G. Localization of Trehalose in Partially Hydrated DOPC

DOI: 10.1021/acs.jpcb.5b06864
J. Phys. Chem. B XXXX, XXX, XXX−XXX

Bilayers: Insights into Cryoprotective Mechanisms. *J. R. Soc., Interface* **2014**, *11*, 20140069.
(18) Westh, P. Glucose, sucrose and trehalose are partially excluded from the interface of hydrated DMPC bilayers. *Phys. Chem. Chem. Phys.* **2008**, *10*, 4110−4112.
(19) Andersen, H. D.; Wang, C.; Arleth, L.; Peters, G. H.; Westh, P. Reconciliation of Opposing Views on Membrane−Sugar Interactions. *Proc. Natl. Acad. Sci. U. S. A.* **2011**, *108*, 1874−1878.
(20) Kapla, J.; Wohlert, J.; Stevensson, B.; Engström, O.; Widmalm, G.; Maliniak, A. Molecular Dynamics Simulations of Membrane−Sugar Interactions. *J. Phys. Chem. B* **2013**, *117*, 6667−6673.
(21) Savitsky, A.; Malferrari, M.; Francia, F.; Venturoli, G.; Möbius, K. Bacterial Photosynthetic Reaction Centers in Trehalose Glasses: Coupling between Protein Conformational Dynamics and Electron-Transfer Kinetics as Studied by Laser-Flash and High-Field EPR Spectroscopies. *J. Phys. Chem. B* **2010**, *114*, 12729−12743.
(22) Bellavia, G.; Giuffrida, S.; Cottone, G.; Cupane, A.; Cordone, L. Protein Thermal Denaturation and Matrix Glass Transition in Different Protein-Trehalose-Water Systems. *J. Phys. Chem. B* **2011**, *115*, 6340−6346.
(23) Marsh, D. Electron Spin Resonance in Membrane Research: Protein-Lipid Interactions from Challenging Beginnings to State of the Art. Euro. Biophys. *Eur. Biophys. J.* **2010**, *39*, 513−525.
(24) Möbius, K.; Lubitz, W.; Savitsky, A. High-field EPR on Membrane Proteins − Crossing the Gap to NMR. *Prog. Nucl. Magn. Reson. Spectrosc.* **2013**, *75*, 1−49.
(25) Cafiso, D. S. Identifying and Quantitating Conformational Exchange in Membrane Proteins Using Site-Directed Spin Labeling. *Acc. Chem. Res.* **2014**, *47*, 3102−3109.
(26) Dikanov, S. A.; Tsvetkov, Y. D. *Electron Spin Echo Envelope Modulation (ESEEM) Spectroscopy*; CRC Press: Boca Raton, FL; 1992.
(27) Schweiger, A.; Jeschke, G. *Principles of Pulse Electron Paramagnetic Resonance*; Oxford University Press: Oxford, England; 2001.
(28) Erilov, D. A.; Bartucci, R.; Guzzi, R.; Shubin, A. A.; Maryasov, A. G.; Marsh, D.; Dzuba, S. A.; Sportelli, L. Water Concentration Profiles in Membranes Measured by ESEEM of Spin-Labeled Lipids. *J. Phys. Chem. B* **2005**, *109*, 12003−12013.
(29) Volkov, A.; Dockter, C.; Polyhach, Y.; Paulsen, H.; Jeschke, G. Site-Specific Information on Membrane Protein Folding by Electron Spin Echo Envelope Modulation Spectroscopy. *J. Phys. Chem. Lett.* **2010**, *1*, 663.
(30) Matalon, E.; Kaminker, I.; Zimmermann, H.; Eisenstein, M.; Shai, Y.; Goldfarb, D. Topology of the Trans-Membrane Peptide WALP23 in Model Membranes under Negative Mismatch Conditions. *J. Phys. Chem. B* **2013**, *117*, 2280−2293.
(31) Dzuba, S. A.; Marsh, D. ESEEM of Spin Labels to Study Intermolecular Interactions, Molecular Assembly and Conformation. In *A Specialist Periodic Report, Electron Paramagnetic Resonance*; Gilbert, C.; Chechik, V.; Murphy, D.M., Eds.; RSC Publishing: Cambridge, U.K.; 2015, Vol. *24*, pp 102−121.
(32) Milov, A. D.; Samoilova, R. I.; Shubin, A. A.; Grishin, Yu. A.; Dzuba, S. A. ESEEM Measurements of Local Water Concentration in D_2O-Containing Spin-Labeled Systems. *Appl. Magn. Reson.* **2008**, *35*, 73−94.
(33) Koch, H. J.; Stuart, R. S. The Catalytic C-Deuteration of Some Carbohydrate Derivatives. *Carbohydr. Res.* **1978**, *67*, 341−348.
(34) Malferrari, M.; Nalepa, A.; Venturoli, G.; Francia, F.; Lubitz, W.; Möbius, K.; Savitsky, A. Structural and Dynamical Characteristics of Trehalose and Sucrose Matrices at Different Hydration Levels as Probed by FTIR and High-Field EPR. *Phys. Chem. Chem. Phys.* **2014**, *16*, 9831−9848.
(35) Konov, K. B.; Isaev, N. P.; Dzuba, S. A. Glycerol penetration profile in phospholipid bilayers measured by ESEEM of spin-labelled lipids. *Mol. Phys.* **2013**, *111*, 2882−2886.
(36) Konov, K. B.; Isaev, N. P.; Dzuba, S. A. Low-Temperature Molecular Motions in Lipid Bilayers in the Presence of Sugars: Insights into Cryoprotective Mechanisms. *J. Phys. Chem. B* **2014**, *118*, 12478−12485.
(37) Doster, W. The Two-step Scenario of the Protein Dynamical Transition. *J. Non-Cryst. Solids* **2011**, *357*, 622−628.
(38) Dzuba, S. A.; Raap, J. Spin-Echo Electron Paramagnetic Resonance (EPR) Spectroscopy of a Pore-Forming (Lipo)Peptaibol in Model and Bacterial Membranes. *Chem. Biodiversity* **2013**, *10*, 864−875.

DOI: 10.1021/acs.jpcb.5b06864
J. Phys. Chem. B XXXX, XXX, XXX−XXX